2

Conf-921281--1

PNL-SA-21677

RECEIVED
JUN 21 1993
OSTI

QUANTITATIVE LUMINESCENCE IMAGING SYSTEM

C. R. Batishko
K. A. Stanl
B. A. Fecht

DISCLAIMER

This report was prepared as an account of work sponsored by an agency of the United States Government. Neither the United States Government nor any agency thereof, nor any of their employees, makes any warranty, express or implied, or assumes any legal liability or responsibility for the accuracy, completeness, or usefulness of any information, apparatus, product, or process disclosed, or represents that its use would not infringe privately owned rights. Reference herein to any specific commercial product, process, or service by trade name, trademark, manufacturer, or otherwise does not necessarily constitute or imply its endorsement, recommendation, or favoring by the United States Government or any agency thereof. The views and opinions of authors expressed herein do not necessarily state or reflect those of the United States Government or any agency thereof.

Presented at the
Workshop on 3-Dimensional
Graphics Modeling of RFR
Distribution in Humans
December 8-9, 1992
Brooks AFB, TX

Prepared for
the U.S. Department of Energy
Contract DE-AC06-76RLO 1830

Pacific Northwest Laboratory
Richland, Washington 99352

MASTER

DISTRIBUTION OF THIS DOCUMENT IS UNLIMITED

QUANTITATIVE LUMINESCENCE IMAGING SYSTEM

C. R. Batishko
K. A. Stahl
B. A. Fecht

Pacific Northwest Laboratory[a]
Richland, Washington 99352

ABSTRACT

The goal of the MEASUREMENT OF CHEMILUMINESCENCE project is to develop and deliver a suite of imaging radiometric instruments for measuring spatial distributions of chemiluminescence. Envisioned deliverables include instruments working at the microscopic, macroscopic, and life-sized scales. Both laboratory and field portable instruments are envisioned.

The project also includes development of phantoms as enclosures for the diazoluminomelanin (DALM) chemiluminescent chemistry. A suite of either phantoms in a variety of typical poses, or phantoms that could be adjusted to a variety of poses, is envisioned. These are to include small mammals (rats), mid-sized mammals (monkeys), and human body parts. A complete human phantom that can be posed is a long-term goal of the development. Taken together, the chemistry and instrumentation provide a means for imaging RF dosimetry based on chemiluminescence induced by the heat resulting from RF energy absorption.

The first delivered instrument, the Quantitative Luminescence Imaging System (QLIS), resulted in a patent, and an *R&D Magazine* 1991 R&D 100 award, recognizing it as one of the 100 most significant technological developments of 1991.

The current status of the project is that three systems have been delivered, several related studies have been conducted, two preliminary human hand phantoms have been delivered, system upgrades have been implemented, and calibrations have been maintained.

a Pacific Northwest Laboratory is operated by Battelle Memorial Institute for the U. S. Department of Energy under contract DE-AC06-76RLO 1830.

Current development includes sensitivity improvements to the microscope-based system; extension of the large-scale (potentially life-sized targets) system to field portable applications; extension of the 2-D large-scale system to 3-D measurement; imminent delivery of a more refined human hand phantom and a rat phantom; RF, thermal and imaging subsystem integration; and continued calibration and upgrade support.

ACKNOWLEDGEMENTS

This presentation describes research and development conducted for the United States Air Force Armstrong Laboratory at the Pacific Northwest Laboratory (PNL), operated by Battelle Memorial Institute for the Department of Energy under DOE Contract DE-AC06-76RLO 1830. The research was conducted as a PNL related services project, PNL 10196/TD2149, MEASUREMENT OF CHEMILUMINESCENCE, in support of the Armstrong Laboratory's RF dosimetry program.

The authors wish to acknowledge the technical contributions of the following individuals without which these results would not have been obtained.

The concept of spatially distributed RF dosimetry exploiting chemiluminescence implemented using the Air Force developed chemistry originated with David N. Erwin and Johnathan L. Kiel, both of the USAF Armstrong Laboratory. Dr. Kiel was responsible for the development of the chemistry.

The M-QLIS was greatly enhanced by a highly efficient, custom RF radiator developed at PNL by Gerald A. Sandness (PNL, Automation & Measurement Sciences).

The phantoms reported were fabricated at PNL by N. Ross Gordon (PNL, Materials Sciences).

PREFACE

This document annotates the accompanying set of graphic materials. The materials are essentially copies of viewgraphs used in a briefing at the 8-9 December 1993 Workshop on 3-Dimensional Modelling of RFR Distributions in Humans, held at the USAF Armstrong Laboratory, Brooks AFB, Texas.

INTRODUCTION

The MEASUREMENT OF CHEMILUMINESCENCE project began in mid-CY85 with a feasibility study of the application of low light level video radiometry to the problem of radiometrically quantifying spatial distributions of chemiluminescent emissions. The intensity of these emissions can be correlated to chemical reaction rates, temperature rise in the sample, and ultimately to absorbed RF energy.

The envisioned temporal resolution of one to ten seconds and sub-millimeter spatial resolution were significant improvements over existing technology involving temporal and spatial integration using photomultiplier tubes (PMT). The delivered temporal and spatial resolution are 1/30 second and approximately 1/4 mm, respectively.

Successful results of the feasibility study led to a continuing effort with the scope of development and delivery of a suite of radiometric instruments for measurement of chemiluminescence. Instruments envisioned included instruments working at the microscopic, macroscopic, and life-sized scales. Both laboratory and field portable instruments were envisioned.

VIEWGRAPH ANNOTATIONS

1. TITLE SLIDE - Quantitative Luminescence Imaging System

The instruments delivered under the MEASUREMENT OF CHEMILUMINESCENCE project have been named Quantitative Luminescence Imaging Systems (QLIS) and will be referred to as such throughout. The variations will be referred to by prefixes as follows:

- M-QLIS microscope-based QLIS
- QLIS the prototype QLIS, being a mid-scale macroscopic system designed for 50 mm diameter sample cells
- L-QLIS large-scale QLIS, further differentiated as 2-D or 3D

The principle PNL contributors to this presentation include C. R. Batishko, K. A. Stahl, and B. A. Fecht. Pacific Northwest Laboratory is a U.S. Department of Energy multiprogram National Laboratory.

2. METHOD OVERVIEW

In the case of cultured organisms, the method begins with RF exposure of the organisms in diazoluminomelanin (DALM), the USAF/AL-developed chemical medium which is key to the chemiluminescence method. The result of the absorption of RF energy by the organisms is to stress the organisms, causing them to produce peroxides, which, in combination with the DALM, results in chemiluminescence. For the current reactions of interest, this light has a spectrum comparable to the standard reaction of luminol in DMSO activated by sodium peroxide, a reaction used as a calibration since its luminous emission as a function of reactant concentrations is known. The spectrum is conveniently broadband, centered in the green to blue-green (~550 nm) region of the spectrum, and somewhat similar to the distribution of sensitivity of the human photopic eye.

The spatial distribution of chemiluminescence is detected by an imaging device - at this time, an intensified video camera of either vidicon-type, or two-dimensional charge coupled device (CCD) array. The detected distribution results in a digitized array which can be displayed as a video frame. With current hardware, the image is 640 x 480 pixels by 8 bits. An 8 bit image is one having 256 gray levels.

The analysis consists of calibrating the gray scale, taking into account:

- spectral distribution of the source
- spectral sensitivity of the camera
- camera gain setting (multiple gain settings are needed to extend the dynamic range of the camera from a fraction of an order of magnitude

represented by 256 gray levels to approximately 3 orders of magnitude, or the equivalent of about 10 bits)

- camera light collection geometry.

The result is a measurement of radiant flux produced by the sample, expressed in photons/sec/cm^2, which can be used to deduce reaction rates, and subsequently used as a dosimetric measurement.

3. IMAGE DETECTION TECHNOLOGY OPTIONS

One of the earliest objectives was to determine if technology existed with adequate sensitivity to detect light below the visual threshold in a way that would be useful in implementing imaging radiometry at this low light level. The initial technology survey found three general classes of image detectors:

- intensified video
- cooled, slow scan, CCDs
- resistive anode encoders

Intensified video detection begins with a photocathode as in a PMT, which converts light (photons) to electrons by way of the photoelectric effect, at a quantum efficiency of tens of percent. In a PMT, the spatially integrated electron flux is multiplied, resulting in measurable, but spatially uncorrelated electric current. Intensified video cameras utilize image intensifiers which maintain the emitted electrons in a spatially correlated distribution as they are multiplied so that the result is an intensified image, not simply a spatially integrated electronic signal.

Modern intensifiers are typically microchannel plate intensifiers. These consist of thin plates comprised of microscopic tubes through which the electrons are drawn by an accelerating potential. The walls of the tubes are coated with materials which absorb electrons, and then emit more electrons than were absorbed. The parallel nature of the tubes results in electrons emitted by the photocathode and entering the plate, maintaining their spatial relationship as they are multiplied though multiple collisions with the walls of the tubes. At the end of the tubes, a shower of electrons emerges from each tube, multiplied by factors of up to hundreds of thousands compared to the numbers entering the tubes. These electrons impinge on a phosphor which

is excited to a higher energy state, then returns to its lower state by emitting light to produce an image whose brightness is related to the amount of light detected by the photocathode, and thus the chemiluminescence emitted by the sample. This intensified image is then detected by a video camera. The QLIS use a high sensitivity vidicon-type camera, while the M-QLIS and L-QLIS use a CCD camera for this purpose.

Cooled, slow scan CCDs have no intensifiers, but derive their sensitivity from long time integration. Whereas intensified video cameras produce images at video frame rates (30 frames/second), cooled, slow scan CCDs produce single frames at temporal resolution limited by the integration time and the time required to transfer the detected image to digital memory. Integration times can be hours, given high-quality CCDs and cryogenic cooling to reduce background noise to a few electrons per detector element per second.

The mechanism at work in CCD cameras is the accumulation of electronic charge in proportion to the amount of light falling on each element of the camera's two-dimensional silicon or gallium arsenide detector array. The array is read out digitally, providing gray scale values which then can be displayed as the image.

The mechanism of the resistive anode encoder also begins with a photocathode, as in the intensified video cameras and PMTs. Typically, high gain is achieved by using a microchannel plate intensifier, as in intensified video cameras. However, final detection and readout is by a different mechanism.

The multiplied and accelerated electron streams leaving the microchannel plate impinge on a flat plate anode. The electrons collected on the plate result in a current that flows to each of four conductors draining four symmetrical quadrants. The current ratios among the conductors is related geometrically to the resistance ratios among the four paths so that the geometrical position at which an electron (or a stream of electrons) impinges on the plate can be computed from simple ratios. By this means, it is possible to achieve sensitivities at the photon counting level, but, conversely, the upper limit of detection is limited by the time discrimination needed to resolve individual events. Apparently simultaneous events, within

the time constant, are recorded as a single event at the centroid of the individual events.

Each method represents advantages and disadvantages relative to the others. The tradeoffs among these, relative to the dosimetry requirements and chemiluminescence characteristics, have guided development choices. Until now, the primary tradeoff has been sensitivity versus cost. Both QLIS and L-QLIS could be implemented at an adequate sensitivity using the lowest cost technology, intensified video. The M-QLIS has demanded much higher ($>10^3$ times) sensitivity so that the more expensive technologies are now under consideration.

As sensitivity has become more important, other factors have become significant. For example, intensified video is widely supported by 8 bit, 30 frame/second hardware and software. Cooled, slow scan CCDs begin at 12 bits, and extend upwards to 20 bits of dynamic range, and result in single images, not a steady stream of 30 frame/sec images. Specialized hardware and software are required. Resistive anode encoders are also time integration devices and also result in high dynamic range, requiring specialized hardware and software. Finally, while intensified video is relatively mature, the other technologies are less so, with cooled, slow scan CCDs just beginning to reach an acceptable level of maturity for relative user friendliness.

4. QLIS - TITLE SLIDE

The first instrument delivered was the QLIS. The line drawing shown in this slide shows the camera assembly installed in the RF waveguide provided by the Air Force. The sample is contained in a cell approximately 50 mm in diameter by 10 mm thick. The cell is mounted in the circular opening shown at the center of the square structure between the two sections of the waveguide. A rigid, L-shaped coherent fiberoptic "image conduit" transfers the chemiluminescence distribution from the cell to the camera assembly mounted above the waveguide.

The light detected is quantified as an 8-bit gray scale value (0 to 255), and used to compute the number of photons emitted per second per square centimeter of the sample using a calibration curve like that shown in this

slide. This curve relates the gray scale value response of the QLIS at each gain setting, to a working parameter which is subsequently associated with the brightness of a National Institute of Standards and Technology (NIST)-traceable calibration standard.

5. QLIS - SYSTEM, AS DELIVERED

The entire QLIS system, as originally delivered, is shown in this slide. The camera/waveguide assembly is shown to the right, along with the supporting computer system. The computer system consisted of a DEC MicroVAX with appropriate video digitizer board and image processing software. The MicroVAX was subsequently replaced with a PC.

6. QLIS - COMPONENTS

The camera section of the QLIS is shown in this slide. At the right is the entire assembly, without the RF source end of the waveguide, and without the square sample cell mounting structure. The camera assembly is shown with the components separated at the center of the slide. The fiberoptic image conduit assembly is shown separated at the left of the slide. The L-shaped fiberoptic conduit is wrapped with black, opaque tape to exclude ambient light. The housing/coupler mechanically couples the L-shaped fiberoptic conduit and the fiberoptic reducer.

Not shown is the QLIS calibration source, a 50 mm diameter radioluminescent source based on carbon-14 exciting a P-20 phosphor. The brightness of the source is known to degrade by about 1% per year, due primarily to aging of the phosphor. (The half-life of carbon-14 is 5,730 years, so radioactive decay is insignificant). The source replaces the sample cell at the input end of the fiberoptic reducer. This source was selected for its low light level short-term stability, convenience of not requiring external power, compactness, and tunability (by phosphor selection) to closely match expected chemiluminescent source spectra. It is a rugged, sealed package meeting appropriate ANSI standards for handing. Its original calibration was traceable to NIST, and the calibration data which feeds into the analysis has been adjusted periodically to compensate for brightness

degradation. Recertification, or at least comparison of results using an alternate calibration device, is appropriate.

7. QLIS - EARLY IMAGERY

This sample imagery illustrates the capability of the QLIS. During development, the camera was tested using a standard chemiluminescence reaction often used to calibrate systems. It consists of luminol in DMSO, which is then activated by the injection of sodium hydroxide. If reagents are in the prescribed concentrations, a known chemiluminescence (expressed in photons/sec) results. In this case, absolute photometry was not needed, so concentrations were not carefully controlled. The resulting chemiluminescence was near to below the visual threshold of the dark adapted eye.

The luminol/DMSO mixture was placed in a 1 cm x 1 cm spectroscopic cuvette positioned at the focal position of the camera. With only a minimal amount of light leaked into the room from a covered flashlight, the camera was set to its maximum gain and the image recorded on VHS video tape. The purpose was to provide a reference image which would define the location of the sides of the cuvette and the meniscus. The frame labeled t_0 was digitized with only this leaked ambient light present in the room. Since the t_1 to t_4 sequence did not have an associated ambient image, the ambient image t_0 was digitized from another test run for use in this presentation. The result is that the meniscus location may not correlate exactly.

Sodium hydroxide was injected using a micropipette and the resulting reaction recorded over a period of a minute or two. Time sequence images t_1 to t_4 were arbitrarily digitized to illustrate the detected chemiluminescence distribution as the reagents produced the initial "flash" which subsequently dimmed. The distribution can be seen to change as the reagents swirled with initial, then decreasing turbulence.

The digitized images were contrast enhanced and pseudocolored for viewgraph clarity, and contrast enhanced for hardcopy clarity. Nevertheless, even the raw video taped imagery clearly shows the swirling action, and the momentary brightening, and subsequent decay of the reaction.

8. QLIS - ANALYSIS

This slide traces the analysis of QLIS data, from detected gray level to resulting radiant flux in photons/sec/cm^2. The camera system detects light using an analog intensified video camera. A frame is "grabbed", meaning it is captured and digitized to an 8-bit gray scale. The 8-bit gray scale value, at a point or averaged over some selected area, is measured using a commercial image processing application, IMAGE PRO PLUS™. The gray scale value is associated with a relative brightness by comparison with a relationship between known brightness and resulting gray scale values at each of a range of intensifier gain settings.

Since the sample emission is invariably different than the camera spectral sensitivity, a normalization factor is defined from the known sample chemiluminescence emission spectrum, the spectral content of the calibration source (filtered to be photopic), and the camera spectral sensitivity.

Using the average gray scale values of the calibration source and measured from the digitized image of the sample chemiluminescence, the spectral normalization factors, and scale factors derived from gray scale values and gain settings, a radiance can be computed for the point or area of interest, from which the gray scale value was measured.

Using the solid angle of the collecting aperture, in this case of the input end of the fiberoptic reducer, the radiance computed in the previous equation, the actual area of the sample represented by one image pixel, and the number of pixels of interest, the radiant flux can be determined.

The result is also expressed in terms of the number of photons/sec/cm^2. To determine this number, the radiant flux is fitted to the relative spectrum of the chemiluminescence. The spectrum is divided into narrow bands (10 nm) and the amount of energy determined for each band. An average photon energy for the band is used to deduce the number of photons required at that energy to produce the radiant flux in the band. For the QLIS, the detection limit is about 2×10^5 photons/sec/cm^2.

9. M-QLIS - TITLE SLIDE

The M-QLIS was the second system delivered. The design objective was to develop a microscope system capable of providing the same kind of video-based imaging radiometry as the QLIS, but using a microscope having a custom, stage-mounted RF antenna. The goal was a tool which would allow researchers to quantify the distribution of chemiluminescence at the cellular level of spatial resolution. This slide lists the subsystems used in assembling the M-QLIS. The system included the following components:

- microscope - Olympus model #BHMJ
- camera - ITT model #F4577
- calibration system - Hoffman Engineering model #RS-65-C Spectral Radiance Standard (NIST traceable)
- computer - Gateway 2000 80486/33 PC-AT compatible
- mass data storage - Alphatronics INSPIRE™ 650 MB erasable optical drive
- frame digitizer - Imaging Technology VS-100/640
- image processing software - Media Cybernetics IMAGE PRO PLUS™
- RF antenna - custom developed and fabricated by PNL

10. M-QLIS/QLIS GRAPHIC

This slide shows conceptual designs of both the QLIS and the M-QLIS. Notice that the artist's conception indicates that the QLIS was intended to measure colonies, while the M-QLIS was intended to measure individual cells (and perhaps intracellular structures).

The M-QLIS consists of a moderate quality research microscope with an intensified video camera and image digitizing and processing computer, RF antenna and RF source. While it was obvious that photometric sensitivity greater than that of the QLIS would be required, it was not clear how much greater it would need to be. Intensified video was again implemented as the lowest cost detection technology, and for its compatibility with the QLIS and processing/analysis technology.

11. M-QLIS SYSTEM

The delivered system consists of the microscope, intensified camera, calibration source, RF antenna, and PC-compatible computer running commercially available image processing software, with some custom routines.

12. M-QLIS - SYSTEM SENSITIVITY

The sensitivity of the system, as delivered, is inadequate for the level of chemiluminescence transmitted through the microscope at any magnification. This table summarizes the detection limit at various magnifications.

A number of camera systems have been tested with the microscope to try to improve sensitivity. Cameras tested include both intensified video and 16 bit cooled, slow scan CCD systems. Only one, a Hammamatsu C2400-47 camera shows promise.

13. M-QLIS - RF ANTENNA

The antenna provided by Armstrong Lab could not be adapted to the requirement. A replacement was designed and fabricated to mount beneath the post-mounted microscope tube and serve as the microscope stage. It was designed to accept two-inch diameter sample dishes which are placed directly above the radiating elements. The entire antenna assembly is mounted on X-Y stages for lateral positioning. Focus is adjusted using the post-mounted tube assembly.

This slide shows the structure of the PNL-designed RF antenna. The radiating elements are coaxial cylinders of brass shaped and positioned so as to provide a high efficiency field over a useful area of the sample dish.

This slide also illustrates the improvement in radiated power of the PNL antenna compared to the older antenna provided by Armstrong.

14. M-QLIS - RF ANTENNA

This slide shows the custom PNL-developed radiator mounted in position below the microscope objectives. Notice that it fits into a recess in the microscope baseplate and includes micrometer drive X-Y translators.

15. L-QLIS TITLE SLIDE

The Large Scale QLIS (L-QLIS) was designed to provide the same kind of quantified imaging radiometry as the QLIS, except for large samples. The system consists of an ITT intensified video camera and a fast f/0.85 Fujinon video camera lens. It is calibrated in the same manner as the QLIS, except that the calibration source is a commercial integrating sphere-type source, rather than a radioluminescent source. A mirror was placed to the left and behind the camera to allow the camera gain control knob and various connectors to be seen.

The two sample images shown on this slide consist of a monochrome, room light, reflected light image of a hollow plastic human hand phantom, and a low light image of the same hand. In the low light image, the chemiluminescence distribution was simulated by loosely inserting cotton swab-like material into the thumb to block the light, and illuminating the entire hand from the back with a very faint, yellow LED. The circular area to the right of the hand in the low light image is the aperture of the calibration source through a stack of neutral density filters. The elongated patches above and to the left of the aperture are light leakage around the filter stack.

16. L-QLIS RADIOMETRY ILLUSTRATED

L-QLIS radiometry is performed identical to the analysis already outlined for the QLIS. This slide illustrates another facet of analysis made possible by the tools included in the image processing software. The reflected light image is shown for geometrical reference. The processed images are all taken from the same digitized frame, but each is processed to isolate areas having gray scale values in a selectable range. This enables the average gray scale value to be found for all pixels in the image which are within that preselected range.

The image at the upper left is a raw low light image. The image at the lower left has had all pixels greater than 128 in the 0 to 255 (8 bit) range replaced by 255 (white) for visualization purposes. Notice that the distribution across the calibration aperture contains pixels in this range. An IMAGE PRO PLUS™ library function easily reports gray scale value range,

average gray scale of those pixels, number of pixels, real area of those pixels and other selectable parameters.

The remaining images at the top and bottom right, respectively, have had pixel values replaced by 255 (white) for the ranges greater than 195 and between 128 and 195, respectively. Notice in the lower right image that there are areas bounded by white which retain the gray values they had in the raw image, meaning that they are outside the selected range of 128 to 195.

Having determined the average gray scale value using this process, the analysis already described would result in the number of photons/sec/cm^2 coming from the area of the hand defined by the selected gray scale range.

17. PORTABLE L-QLIS

The next step in the development is to adapt the L-QLIS to field operation by using the same camera and lens combination as in the L-QLIS, but with either a VCR for image collection with post-processing at a base station or with a portable computer. While a laptop computer is shown, work is underway to adapt a notebook computer for frame grabbing using a custom, miniaturized frame grabber which doesn't require an expansion slot.

In addition to the computer and camera, a portable system would include a DALM-filled phantom and a portable, ambient light excluding enclosure, represented by the black background shape behind the phantom.

18. 3-D L-QLIS - RATIONALE

Another facet of the development is aimed at adapting the L-QLIS to volume operation. At present, the system maps the light emitted by the volume into a two-dimensional distribution in which the chemiluminescence along a line-of-sight path through the volume is recorded at a single pixel in the 2-D array. Since real organisms are volume objects, a true 3-D volume array of the chemiluminescence distribution is needed.

19. 3-D L-QLIS - CONCEPT

A number of technologies are being considered to implement a 3-D L-QLIS. These include both single and multiple camera technologies.

Since the phantom is transparent to visible light, emitted photons leave their point of origin and travel outward in all directions in straight lines (except for refraction at interfaces and scattering). Simple two or more camera tomography may allow adequately accurate brightness mapping using well-established tomographic algorithms. A commercial software product, IMAGE ANALYST™, implements this kind of technology.

Another approach which was identified earlier in the project and has since been introduced in the literature is somewhat equivalent to confocal microscopy, except on a macro scale. A camera (and its lens system) are characterized to obtain its three-dimensional transfer function. Data acquisition consists of scanning through focus so that the in-focus image moves through the volume from front to back (or vice versa). For one frame at each of a set of image frames, the transfer function is used to deconvolve the image to separate the in-focus light from the out-of-focus light. The in-focus light is then a slice of the volume showing the distribution of radiant emission in the plane of that slice.

A commercial product, MICROTOME™, uses this concept to sharpen and increase depth of field in microscope images.

20. PHANTOMS

The objective of the Phantoms Task is to develop and deliver a series of mammal phantom shells which would be filled with the DALM solution for use in research. The phantoms would include human body part models, including hands, limbs and head; rats; chimps; and possibly others. The culmination of the research will be a life-sized human phantom.

Phantoms will provide a capability for the researcher to select various poses, either through poseable joint designs or through various phantoms representing standard poses. For example, rat phantoms would be delivered in both upright and normal positions. For the human phantom, the limb development will precede the completely integrated phantom. Leak-resistant,

movable joints will first be developed, then integrated to form a complete human phantom.

The two hand phantoms shown are the first two delivered phantoms. They are shown in greater detail in subsequent slides.

21. THICK WALL HAND PHANTOM - SIDE

The shape of interest in this case is the hand itself. Ideally, if the DALM could be suspended in the correct shape in free space, the shell would not be needed. However, since it can't, the next best solution is to use a structure to contain the DALM. If the container does not affect the distribution of RF energy, its outer shape can be arbitrary. With this in mind, a cylindrical outer shell was used to enclose a hand-shaped cavity. As can be seen, there is considerable spatial detail which would result in significant optical scatter at the interface. The interfaces between the multiple pourings of the plastic are also evident and would likewise cause unwanted refraction, scattering and reflection at interfaces. A fill hole is located in the top of the cylinder.

22. THICK WALL HAND PHANTOM - BACK

This slide shows the back of the hand in the same phantom as shown in the previous slide.

23. THICK WALL HAND PHANTOM - IRRADIATED

This slide shows the thick-walled phantom, filled with DALM, being irradiated in a cylindrical waveguide. The bright parts of the image are due to chemiluminescence resulting from absorption of RF radiation.

24. THIN WALL HAND

After considering the geometry in terms of its effects on both optical and RF transmission, it was decided that a thinner wall would be preferred, even though the external shape is of no interest. This slide shows a thin-wall hand. As with the thick-wall hand, there is still too much surface detail. The wall thickness varies from one or two millimeters to very thin.

In fact, some areas were so thin that the hand was exceptionally fragile and was accidentally broken. The fill hole is again at the wrist, and the hand would be used with the fingers pointed down. Breakage suggested that a thicker hand was needed. A hand with a thickness of two to three millimeters, with a more polished interior surface to reduce optical scatter, is the next objective.

25. PHANTOM - MATERIALS

The selection of materials for the phantom is crucial. This slide shows the primary requirements of the materials, the range of materials which were tested, and the materials which are in current use. DALM attacks some plastics. For example, the cyanoacrylates (super glue) are destroyed by DALM in a short time, even though the DALM is at a very low concentration in water. The materials need to be optically transparent, with good optical quality to minimize scatter, transmission losses, distortion, etc. The same applies for RF energy since a uniform incident field is required. Keep in mind that it is the DALM solution which is the phantom. The plastic is only the container, and should be as transparent as possible.

26. PHANTOMS - CURRENT/NEAR FUTURE

The phantom development program has resulted in delivery of a thick-(cylindrical) wall hand phantom and a thin-wall hand phantom. Future phantoms are expected to be two to three millimeters thick, in general. Human limbs are planned in the near future, with the next human part perhaps being another hand, then perhaps a head. One or more rat phantoms are planned with at least one having an imbedded, actual skeleton.

27. UPGRADES

As the number of delivered systems increases, the task of upgrading becomes more costly and more important. Upgrades focus on function and compatibility.

Camera sensitivity, in particular, for the M-QLIS is a pressing issue since research based on microscopic absorption measurements is of interest.

Cameras, digitizers, and software compatible with a greater dynamic range is of interest to allow intraframe measurement of both high absorption and threshold absorption.

With several QLIS systems, thermal monitors and controls, RF energy monitors and controls, and peripherals, integration of subsystems into a system controlled from a single computer, perhaps using LABVIEW™-like interfaces, is advantageous, for both operator convenience and data integration. To further facilitate interconnection of a range of output peripherals and mass storage devices, local networking as a work group is being implemented.

For practical field dosimetry, systems, including phantoms, must be portable. One current task focuses on providing a field-portable system based on a notebook computer and including a phantom, ambient light excluding enclosure, and shipping containers.

Computing power and speed are always issues. Within reason, as there is a functional need for a change, high-end PCs and components replace older, slower equipment.

28. SUMMARY

This slide summarizes the systems and phantoms delivered to date, the categories of hardware which have been upgraded, and the focus of the current development.

REFERENCES

Aitken, G. J. M., and P. F. Jones. 1990. "Three-Dimensional image Capture by Volume Imaging." In *Sensing and Reconstruction of Three-Dimensional Objects and Scenes*, vol. 1260, ed. Bernd Girod, pp. 2-9. 15-16 February 1990, Santa Clara, CA. SPIE-The International Society for Optical Engineering.

Automatix. *Image Analyst*. Product Brochure. Automatix, Billerica, MA.

Batishko, C. R. and K. A. Stahl. 1988. *Microscope-Quantitative Luminescence Imaging System (M-QLIS) Description and User's Manual*. PNL-7821, Pacific Northwest Laboratory, Richland, Washington.

Batishko, Charles R., Kurt A. Stahl, David N. Erwin and Johnathan L. Kiel. 1990. "A Quantitative Luminescence Imaging System for Biochemical Diagnostics." *Review of Scientific Instrumentation* 61(9):2289-2295.

Engelhardt, K. and Gerd Häusler. 1988. "Acquisition of 3-D Data by Focal Sensing." *Applied Optics* 27(22):4684-4689.

Erwin, David N., Johnathan L. Kiel, Charles R. Batishko, and Kurt A. Stahl August 1990. "Quantitative Luminescence Imaging System." U.S. Patent 4,948,975.

Kiel, Johnathan L., Gerald J. O'Brien, David M. Simmons, and David N. Erwin. 1989. "Diazoluminomelanin: A Synthetic Electron and Nonradiative Transfer Biopolymer." In *Charge and Field Effects in Biosystems-2*, eds. M. J. Allen, S. F. Cleary, and F. M. Hawkridge, pp. 293-300. Plenum Publishing Corporation, New York.

Kiel, Johnathan L., Gerald J. O'Brien, Jerry Dillon, and John R. Wright. 1990. "Diazoluminomelanin: A Synthetic Luminescent Biopolymer." *Free Radical Research Communications* 8(2):115-121.

Kiel, Johnathan L. and Gerald J. O'Brien March 1991. "Diazoluminomelanin and a Method for Preparing Same." U.S. Patent 5,003,050.

Lee, J. and H. H. Seliger. 1972. "Quantum Yields of the Luminol Chemiluminescence Reaction in Aqueous and Aprotic Solvents." *Photochemistry and Photobiology* 15:227-237.

Seaman, Ronald L., Everette C. Burdette, and Robert L. Deheen. 1989. "Open-Ended Coaxial Exposure Device for Applying RF/Microwave Fields to Very Small Biological Preparations." *IEEE Transactions on Microwave Theory and Techniques* 57(1):

Stahl, K. A. and C. R. Batishko. 1988. *Quantitative Luminescence Imaging System Description and User's Manual*. PNL-6592, Pacific Northwest Laboratory, Richland, Washington.

QUANTITATIVE LUMINESCENCE IMAGING SYSTEM

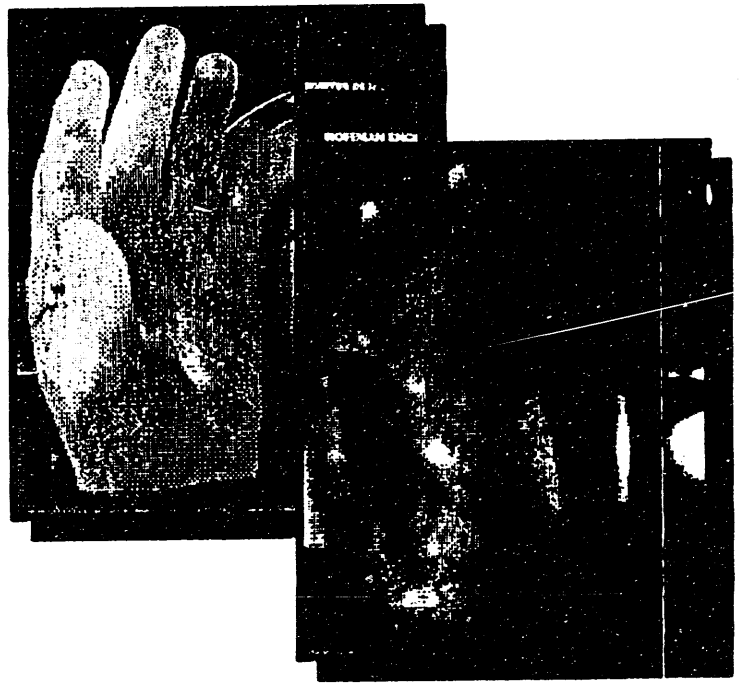

CR Batishko

KA Stahl

BA Fecht

US DOE/Pacific Northwest Lab

crb/EOS/11.8.92

RF

↓

ORGANISMS+DALM

↓

VISUAL SPECTRUM LIGHT

↓

DISTRIBUTION DETECTION

↓

ANALYSIS

cb/EOS/11.6.92

IMAGE DETECTION...

	INTENSIFIED VIDEO:	COOLED, SLOW SCAN, CCD:	RESISTIVE ANODE ENCODER:
COST	$10k-25k	$15k-50k	>$75k
SENSITIVITY	mid 10^{-7}	mid-high 10^{-9}	high $<10^{-9}$
DYNAMIC RANGE	8-bits	12-16 bits	unlimited?
IMAGE FILE FORMAT COMPATIBILITY	standard	special	special
FRAME RATE	video	integrated	integrated
MATURITY	off-the-shelf	state-of-art	moderate

cb/EOS/11.8.92

QLIS

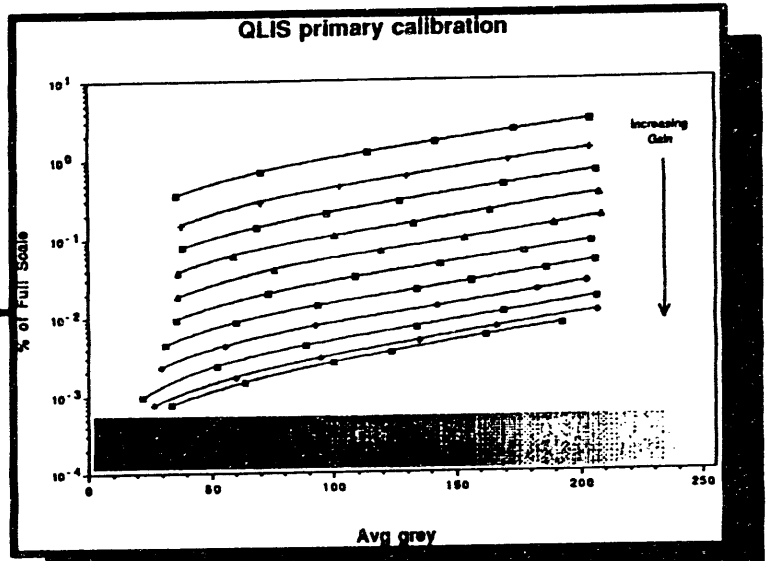

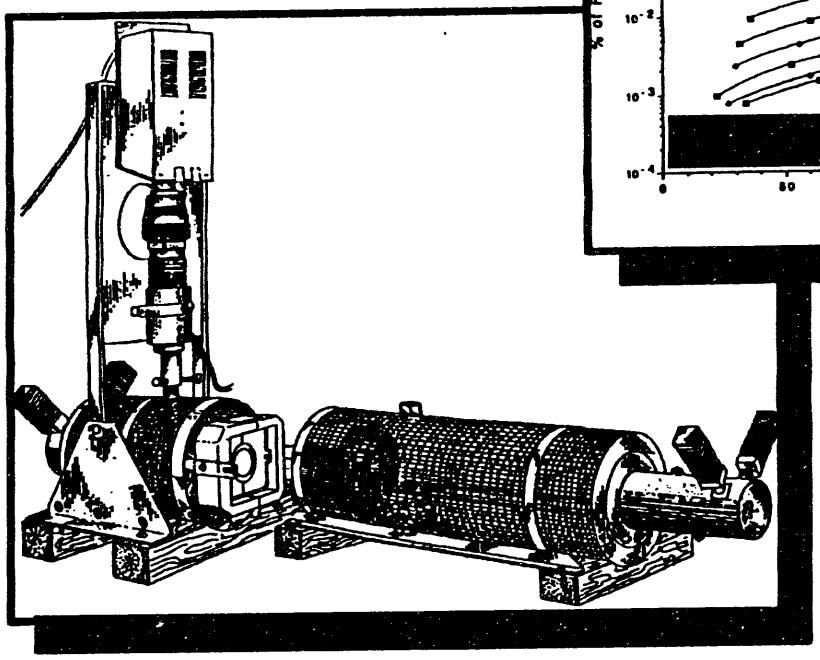

US Patent 4,948,975

R&D

R&D Magazine

crb/EOS/11.10.92

87B040-23CN

5

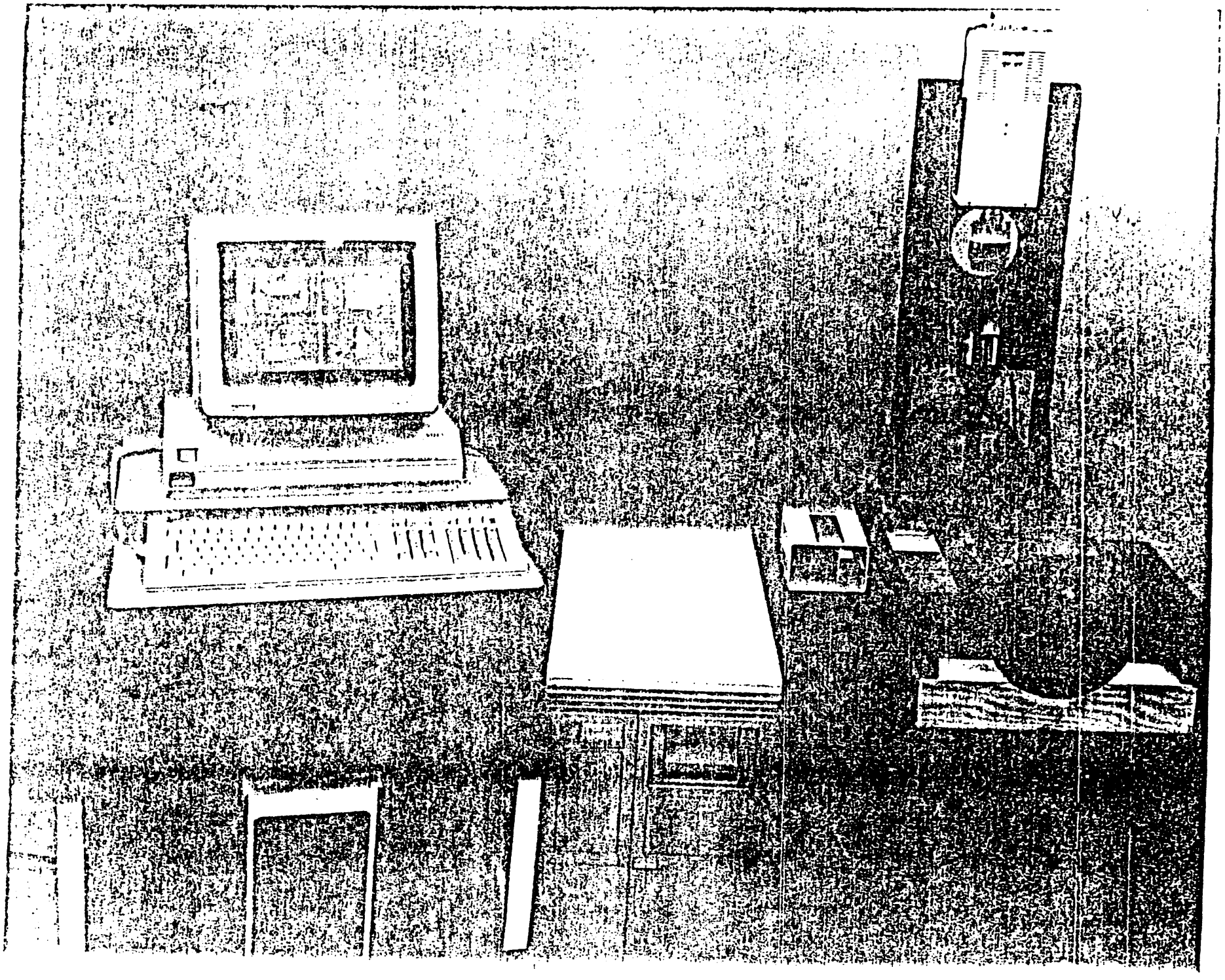

QLIS

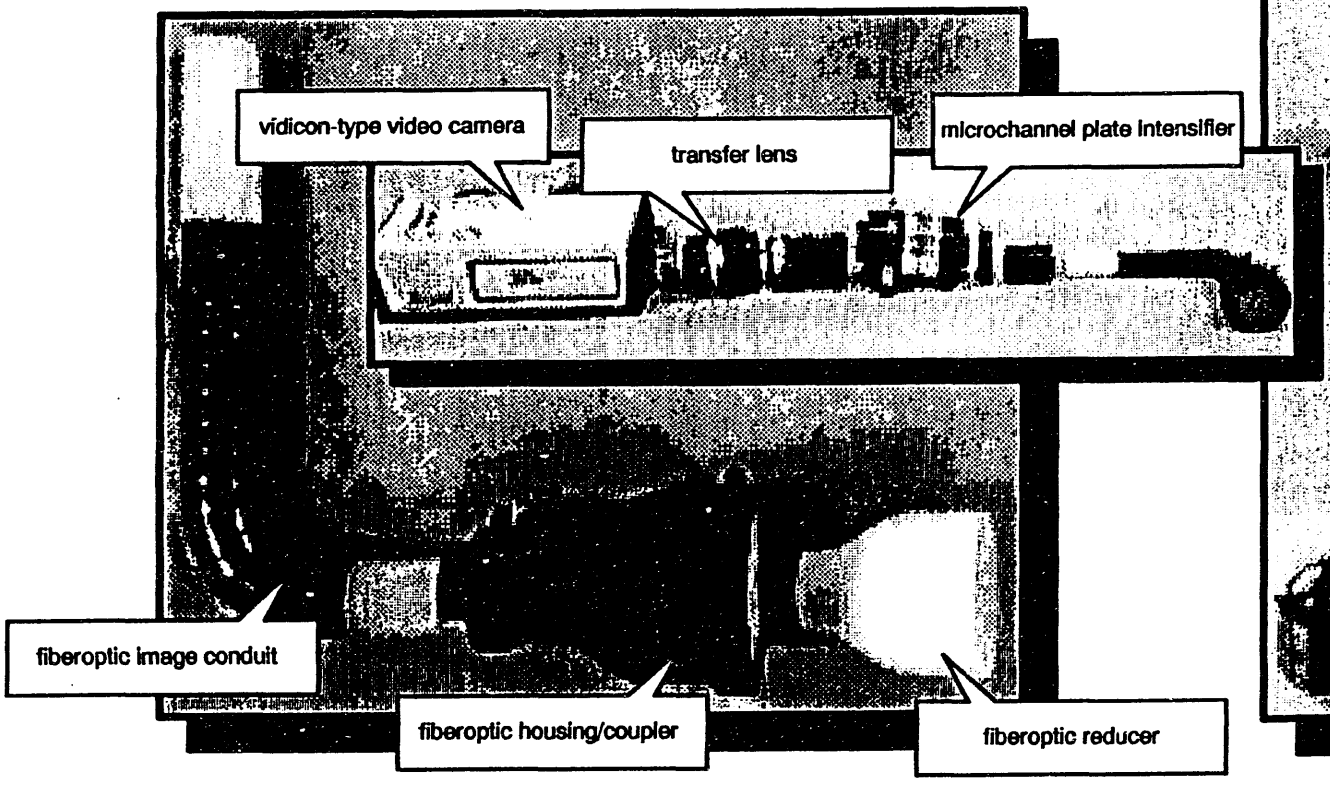
vidicon-type video camera
transfer lens
microchannel plate intensifier
fiberoptic image conduit
fiberoptic housing/coupler
fiberoptic reducer

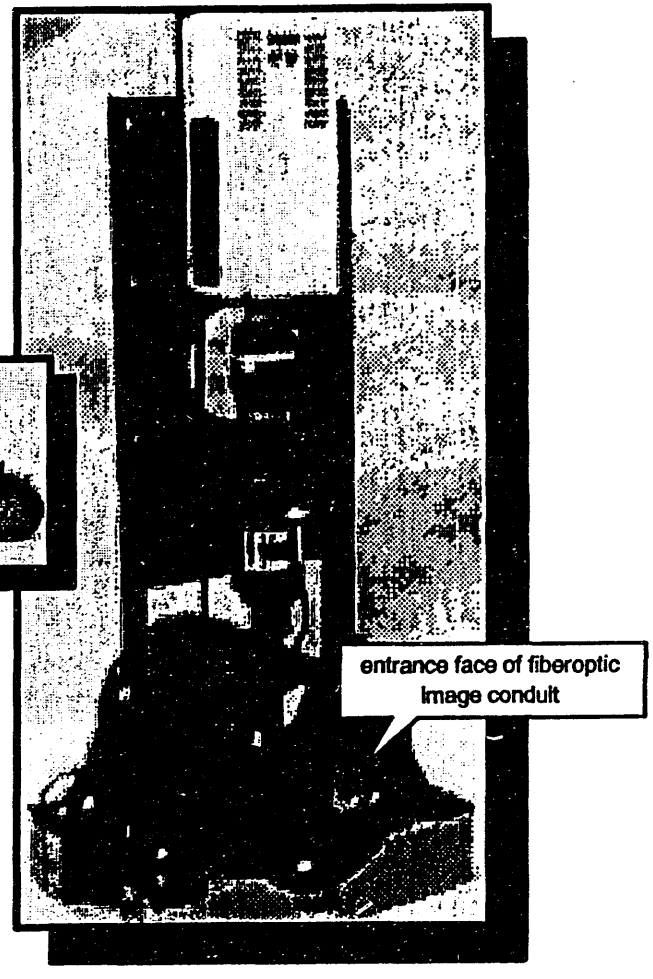
entrance face of fiberoptic image conduit

CHEMILUMINESCENCE

(LUMINOL IN DMSO, IN 1 CM X 1 CM CUVETTE, ACTIVATED WITH SODIUM HYDROXIDE)

SELECTED FRAMES FROM VIDEO RATE RECORD

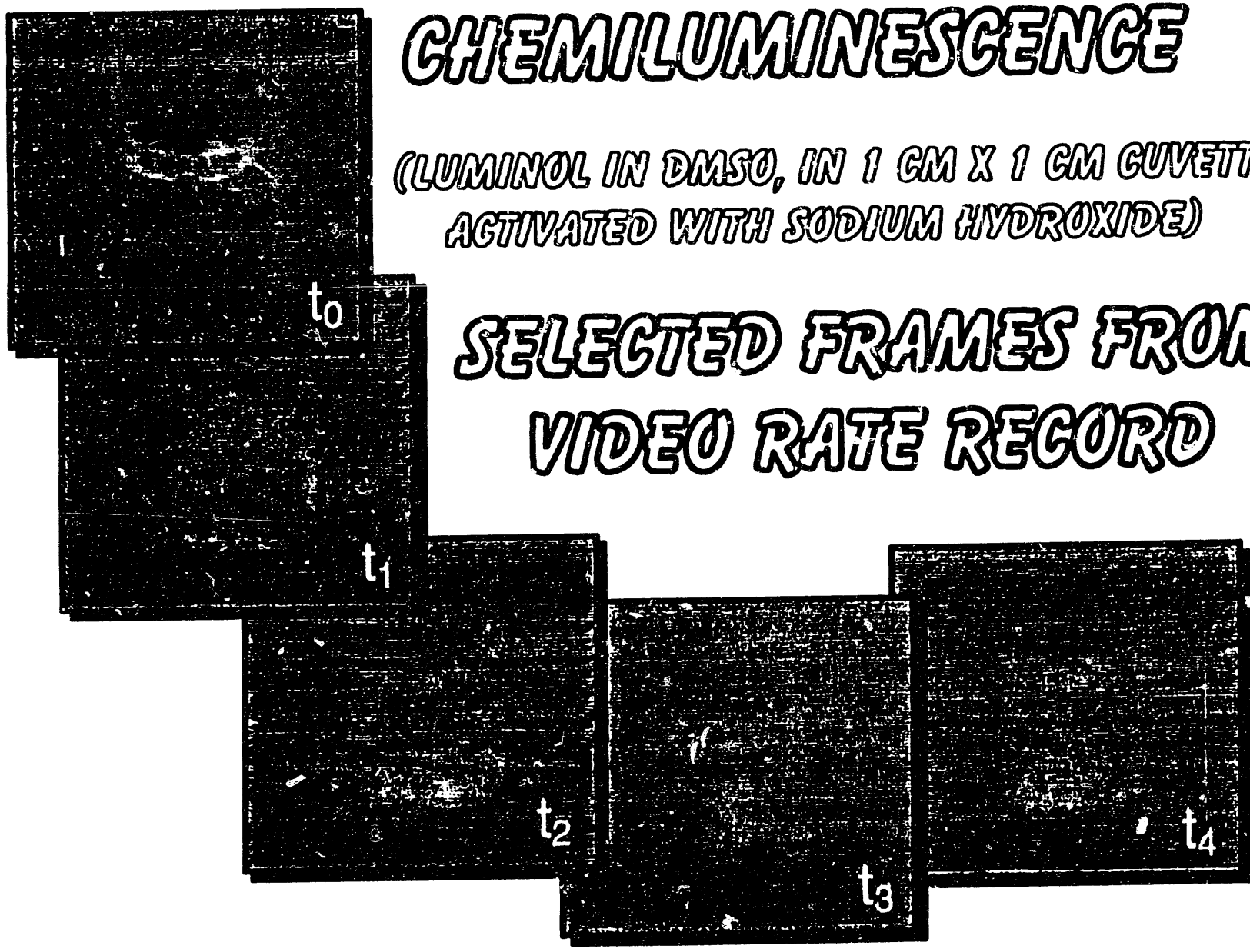

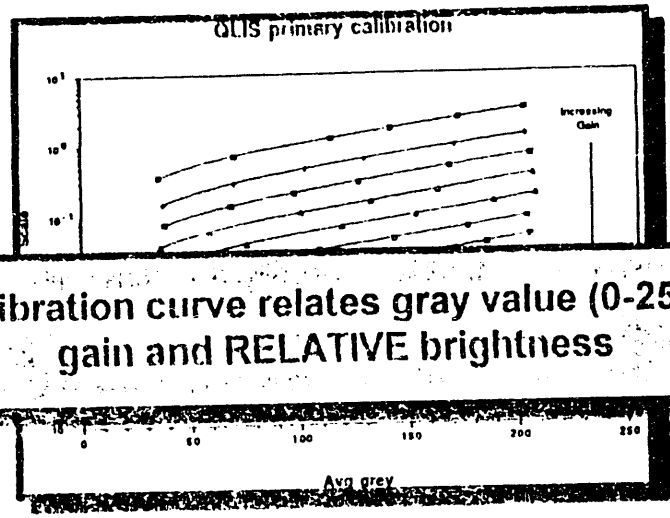

calibration curve relates gray value (0-255), gain and RELATIVE brightness

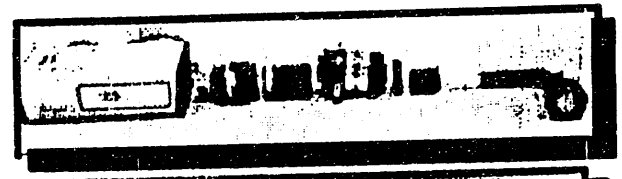

8 BIT DETECTION...

QLIS

normalize for camera spectral response and sample emission spectrum

$$\eta_c = \frac{\int_{\lambda_1}^{\lambda_2} Q(\lambda)\, C(\lambda)\, d\lambda}{\int_{\lambda_1}^{\lambda_2} C(\lambda)\, d\lambda} \qquad \eta_s = \frac{\int_{\lambda_1}^{\lambda_2} Q(\lambda)\, S(\lambda)\, d\lambda}{\int_{\lambda_1}^{\lambda_2} S(\lambda)\, d\lambda}$$

RADIANCE equation:

$$L = [V_S\, s(v_S, g_S)\, \eta_c L_C] / [V_C\, s(v_C, g_C)\, \eta_s]$$

SOLID ANGLE equation:

$$\Omega = 4\pi \sin^2[\tfrac{1}{2}(\sin^{-1} N.A.)]$$

RADIANT FLUX equation:

$$P = LAn\Omega$$

PHOTONS/SECOND equation:

$$N_{ph}(\lambda) = F(\lambda) P / E_p(\lambda)$$

where...

$$F(\lambda) = \frac{\int_{\lambda_n}^{\lambda_{n+10}} S(\lambda)\, d\lambda}{\int_{\lambda_1}^{\lambda_2} S(\lambda)\, d\lambda}$$

results

2×10^5 PHOTONS/SEC/CM^2

ctb/EOS/12.15.92

M-QLIS

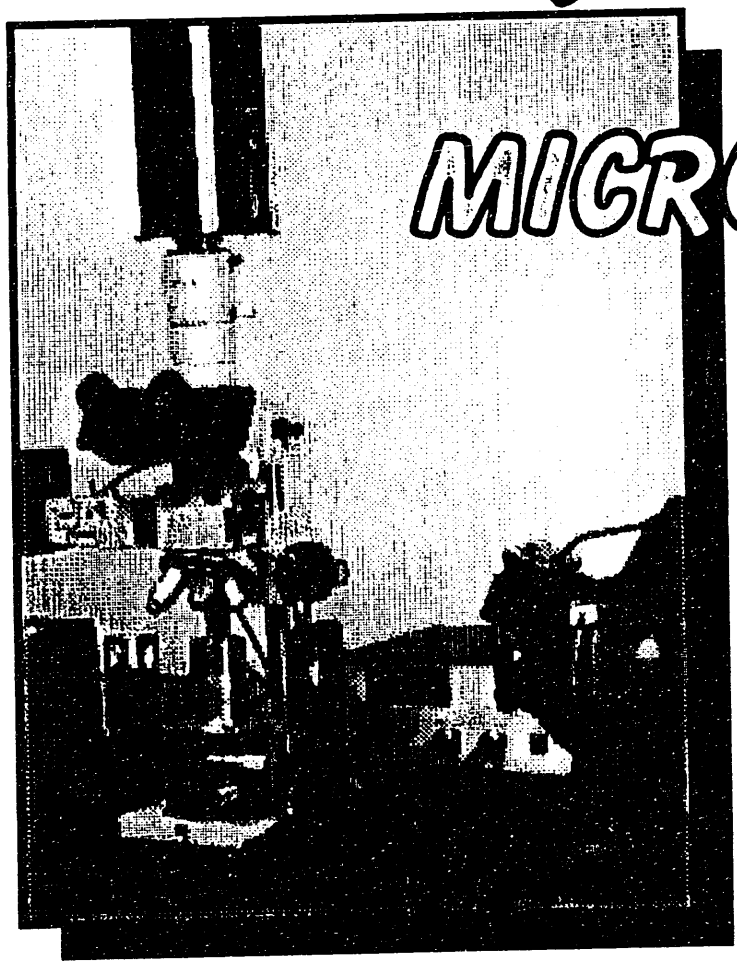

MICROSCOPE-QLIS

Olympus post-mounted microscope

ITT intensified video camera

NIST traceable calibration standard

Gateway 2000 486/33 PC-AT computer

650 MB erasable optical drive

640x480 pixel frame grabber

IMAGE PRO PLUS™ software

PNL developed custom RF radiator

91080602-5C2

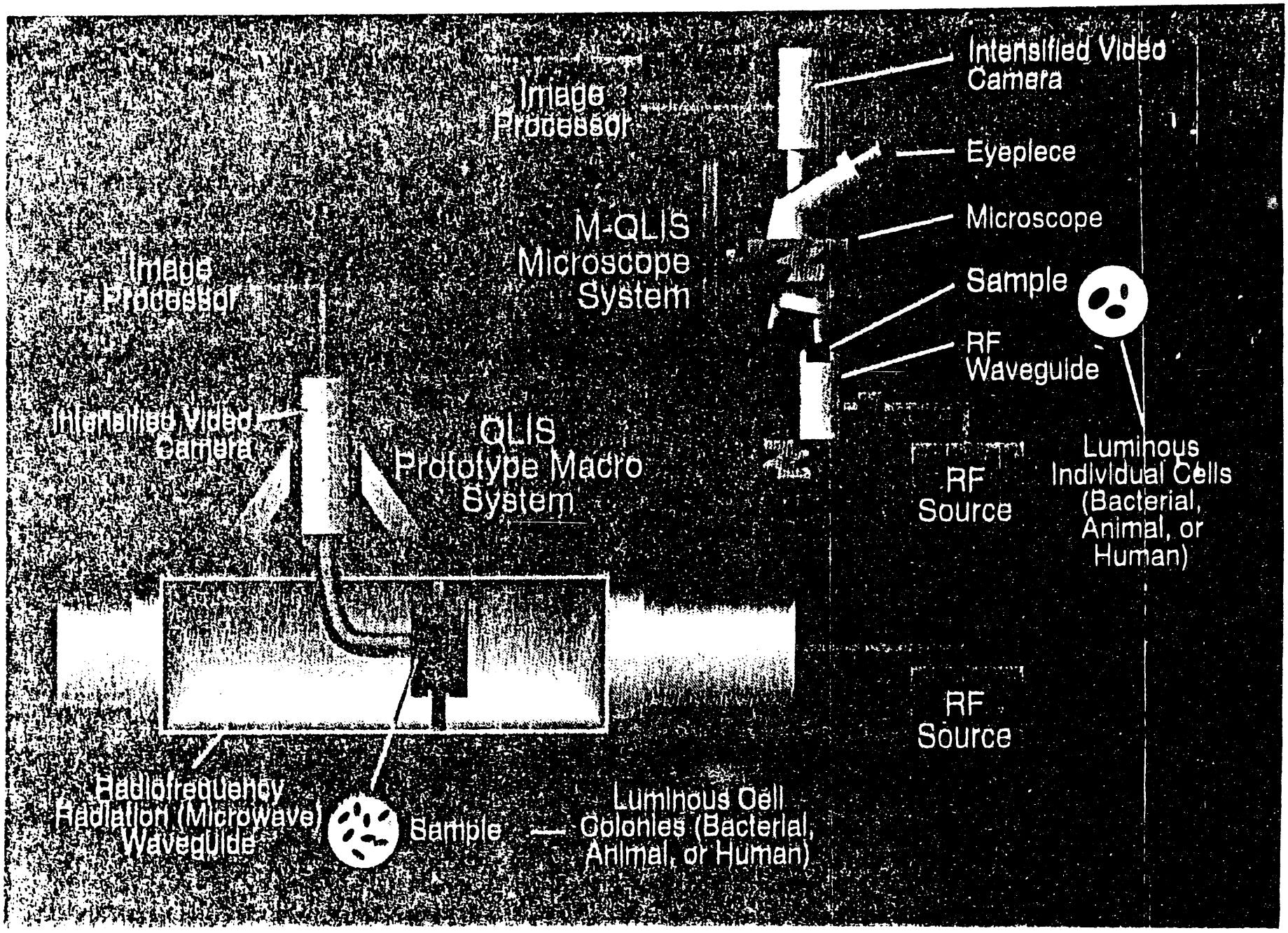

91051026-13

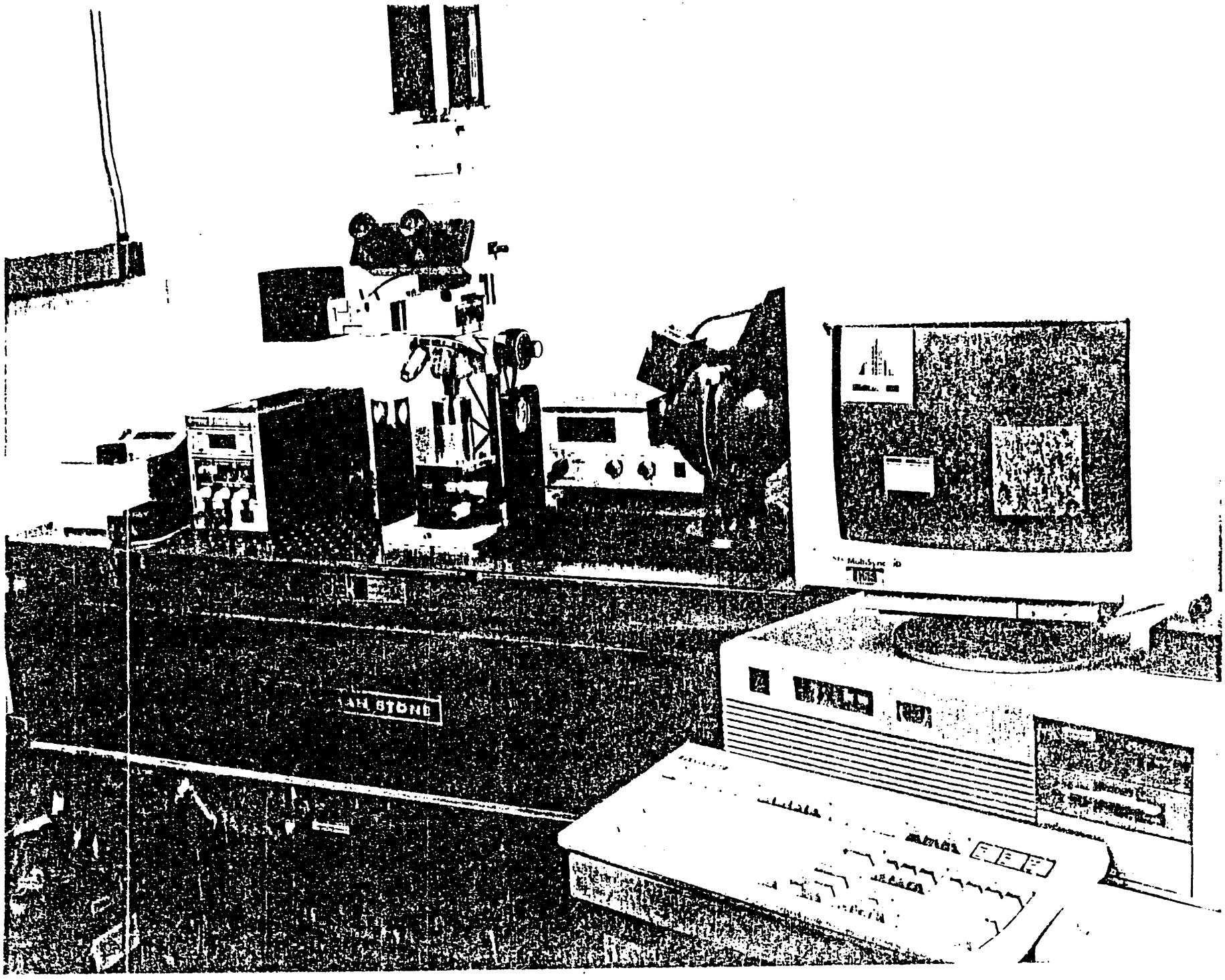

M-QLIS

RADIOMETRIC DETECTION LIMIT

2.5X	8×10^{7} PHOTONS/SEC/CM^2
5X	1×10^{8} PHOTONS/SEC/CM^2
10X	2×10^{8} PHOTONS/SEC/CM^2
20X	9×10^{8} PHOTONS/SEC/CM^2
50X	2×10^{10} PHOTONS/SEC/CM^2

M-QLIS

PNL DEVELOPED CUSTOM RADIATOR

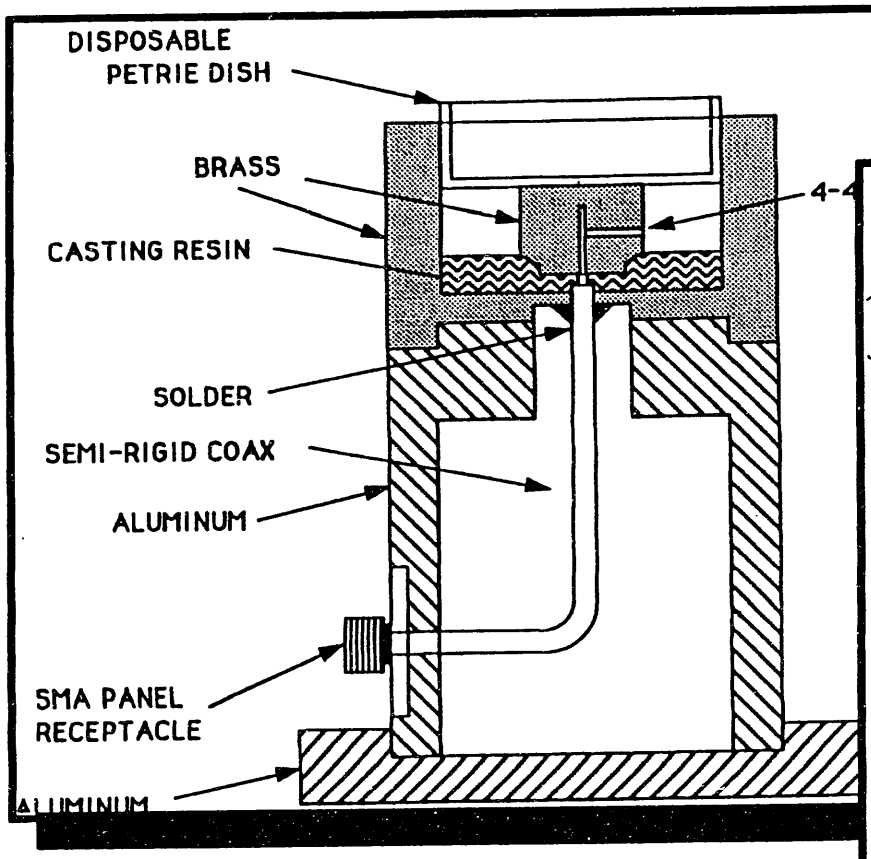

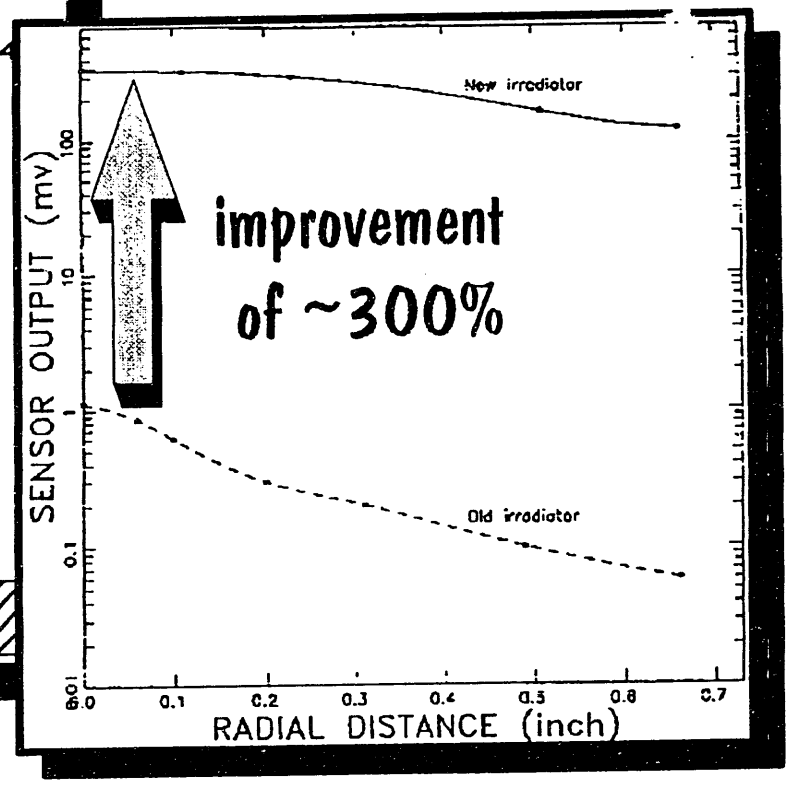

9105 1026-10CN

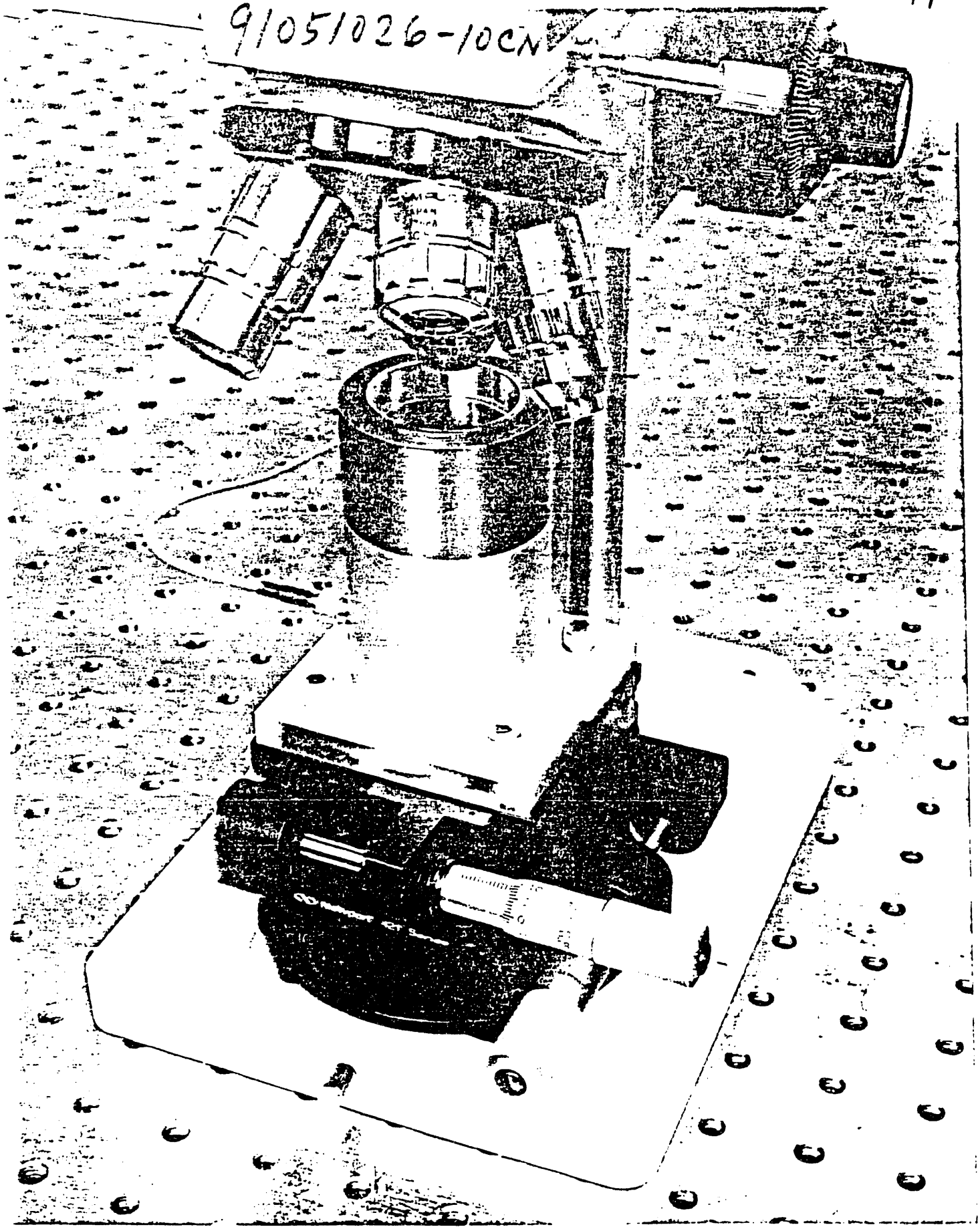

L-QLIS...

LARGE-SCALE QLIS

ITT INTENSIFIED CAMERA
FUJINON 25 MM. F/0.85 LENS

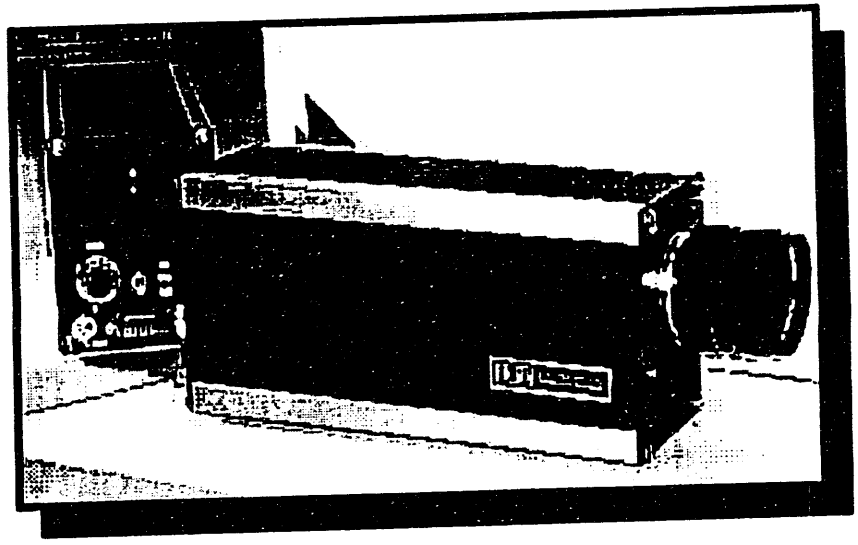

crb/EOS/11.20.92

L-QLIS - IMAGE RADIOMETRY

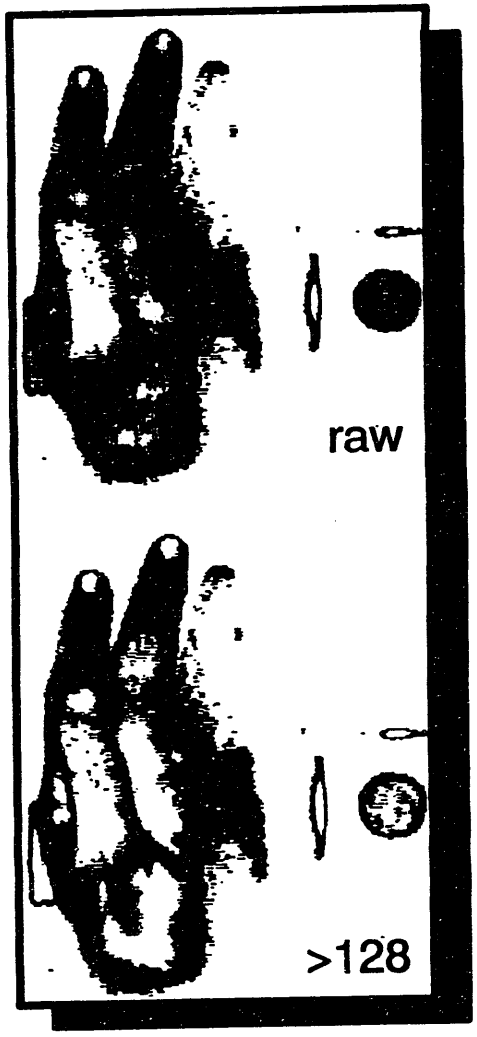

LOW LIGHT THRESHOLDED

REFLECTED LIGHT

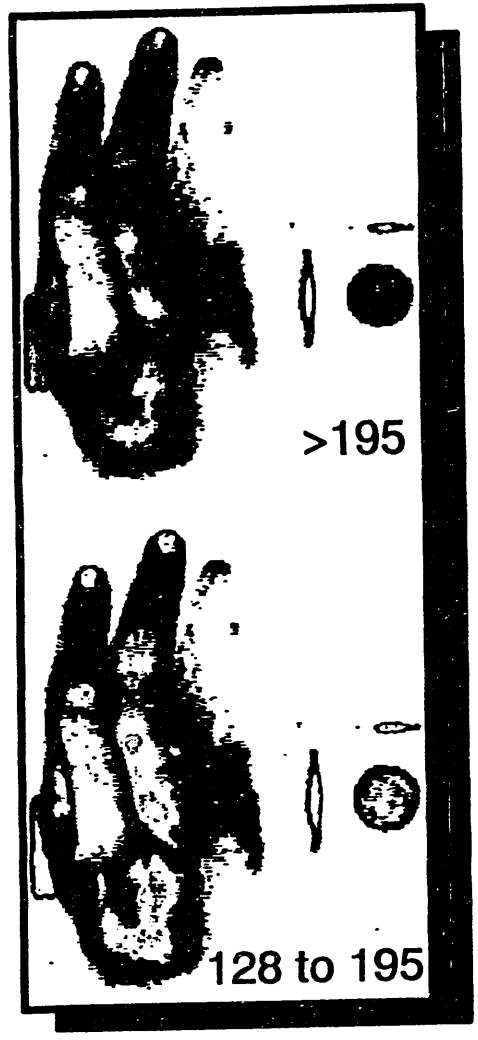

PORTABLE L-QLIS

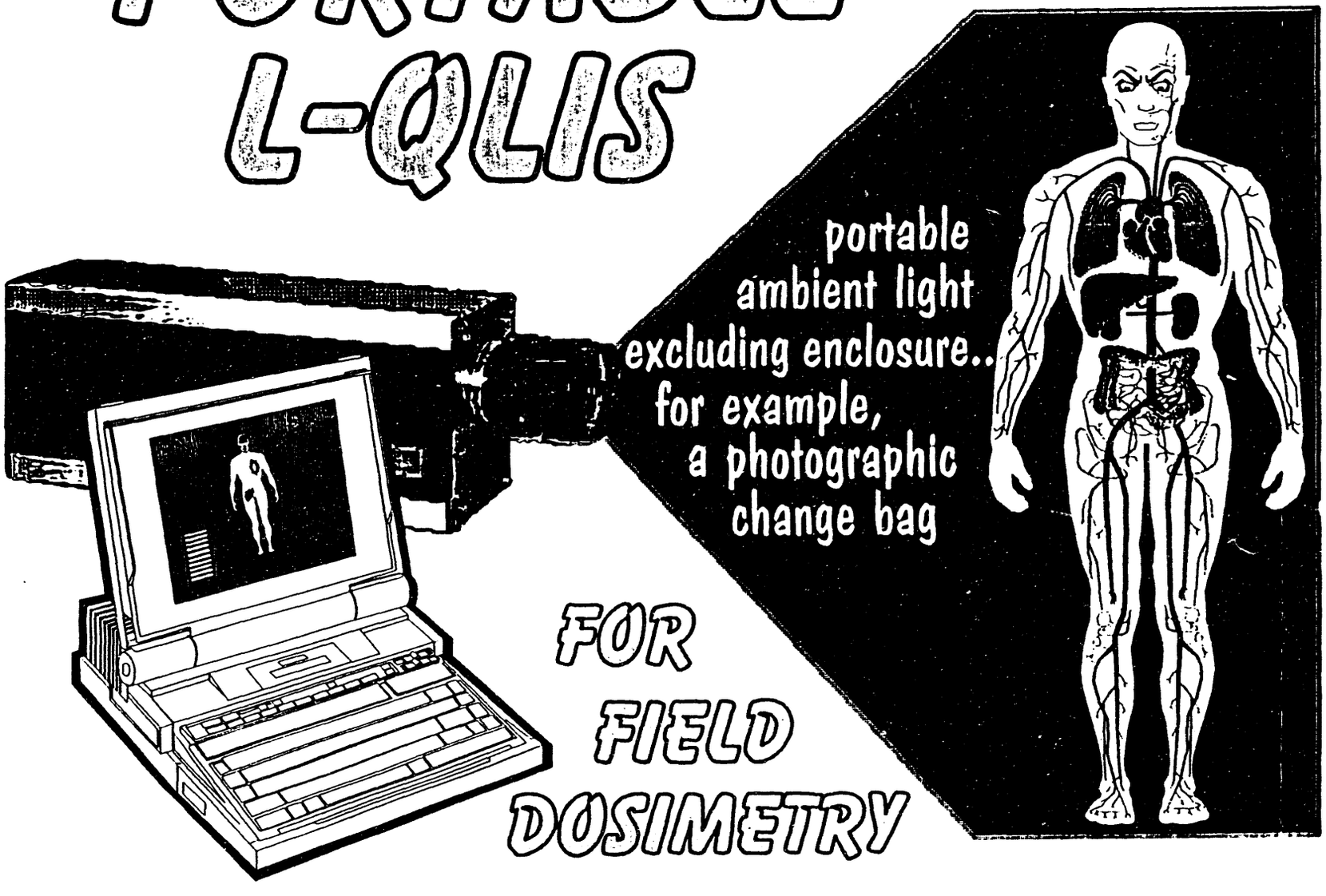

FOR FIELD DOSIMETRY

ob/EOS/12.2.92

L-QLIS...3-D

to map
volumetric chemiluminescence distributions
into a three-dimensional dataset

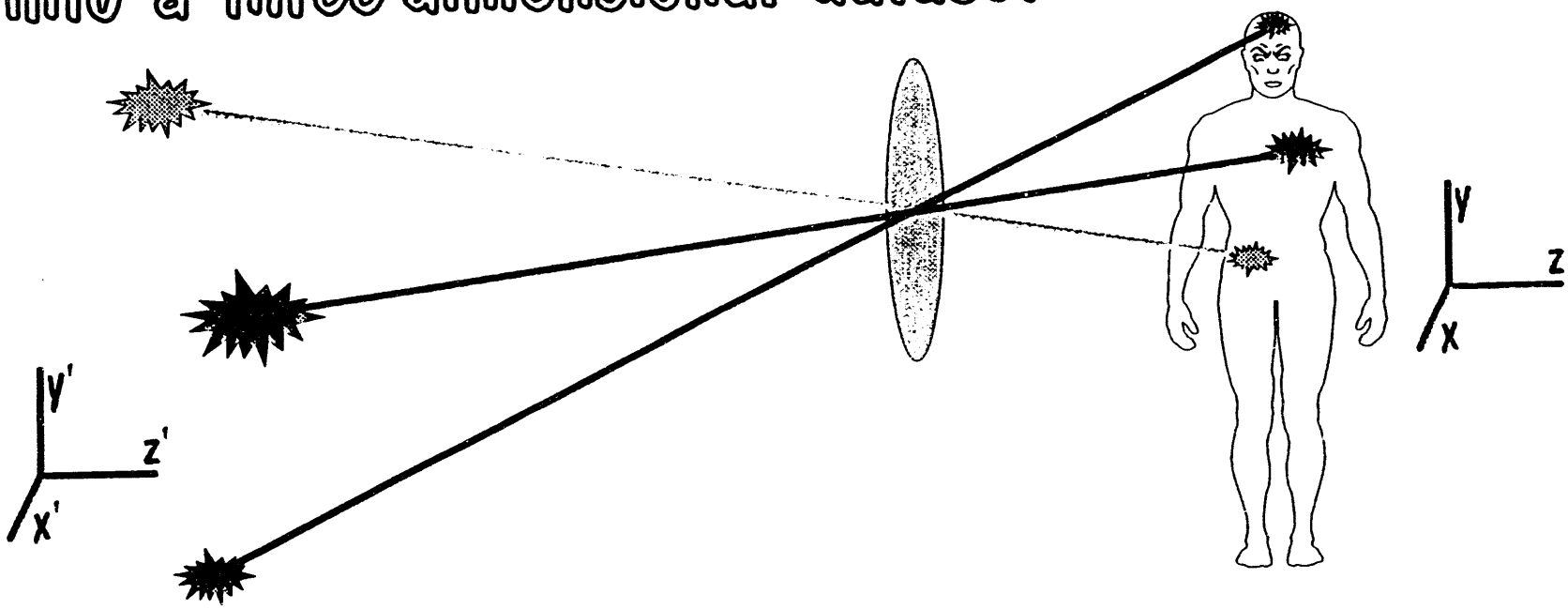

cb/EOS/12.2.92

L-QLIS...3-D

- multiple cameras (IMAGE ANALYST™ on Macintosh)
- focal scanning with defocus removal (MICROTOME™)
- rotating phantom, single camera
- other tomography?

PHANTOMS

FULL-SIZE HUMAN
HUMAN PARTS
RATS
CHIMP
OTHERS?

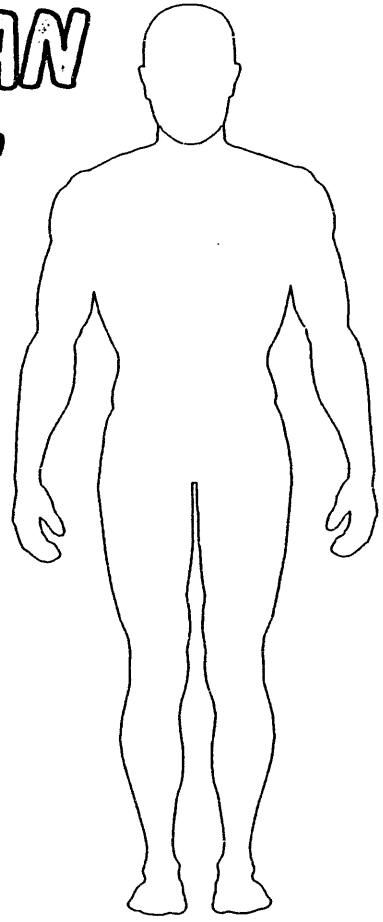

cb/EOS/12.2.92

91122313 -3 CN

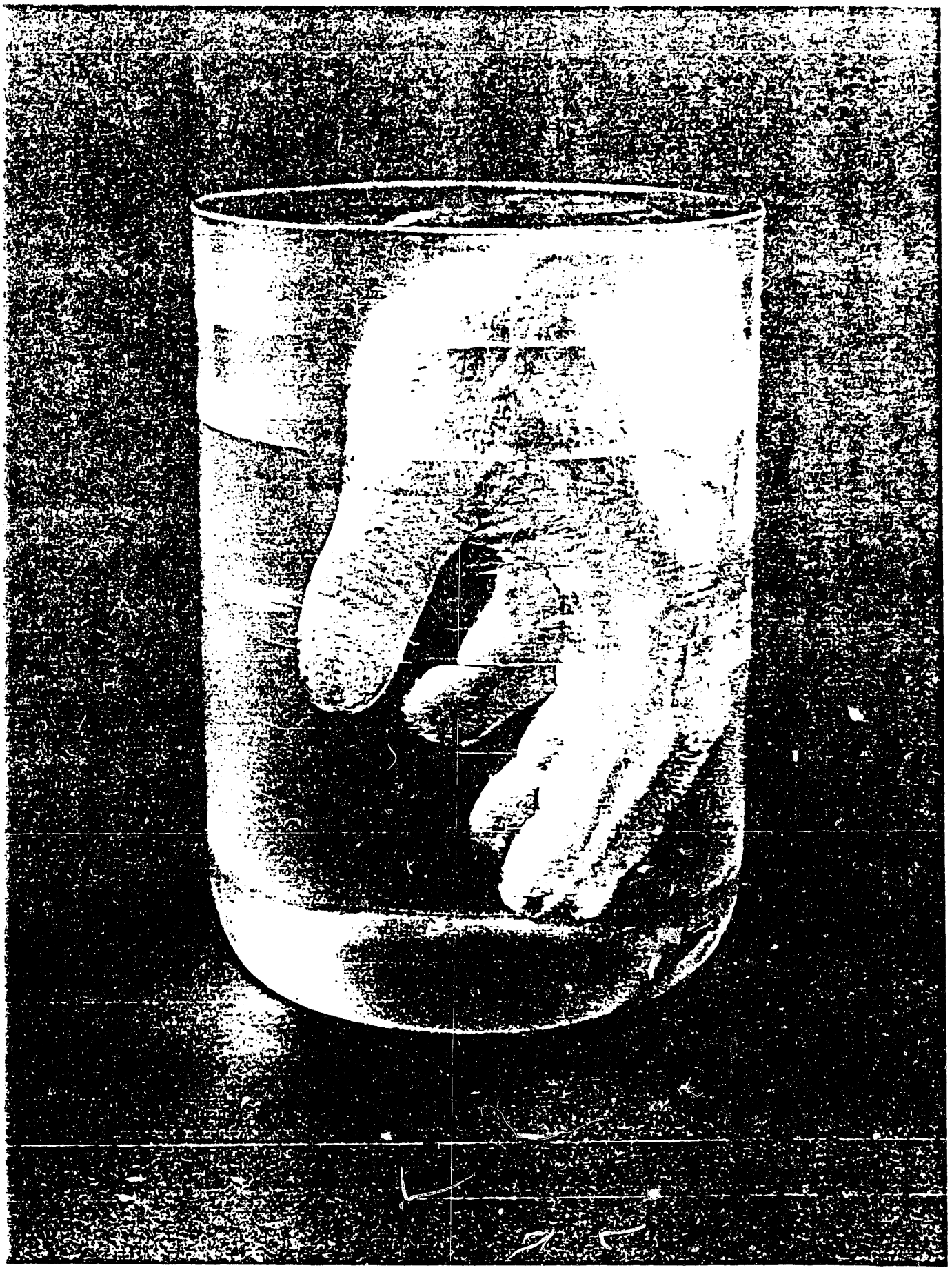

91122-313 - 2CN

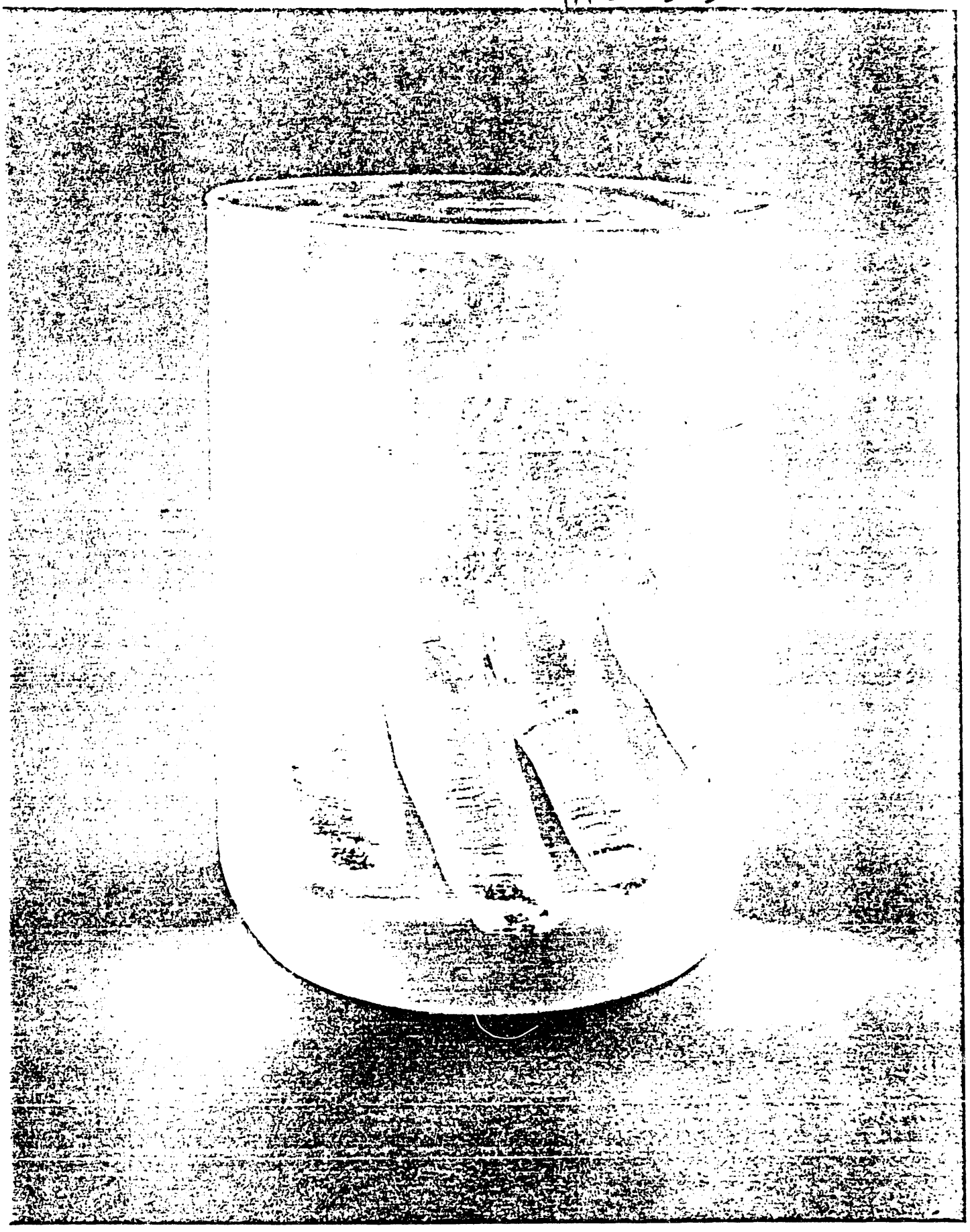

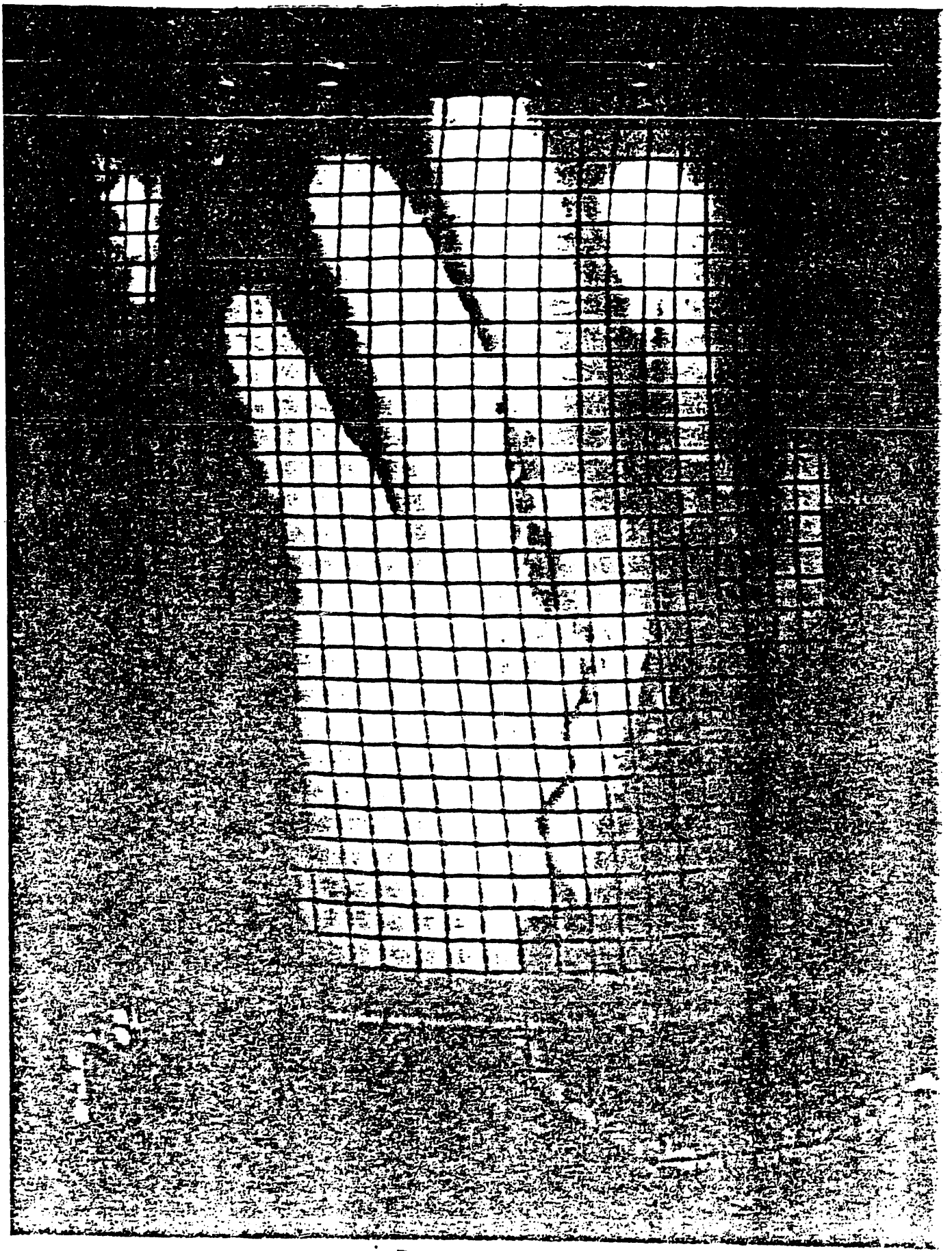

92112042 - ICN

23

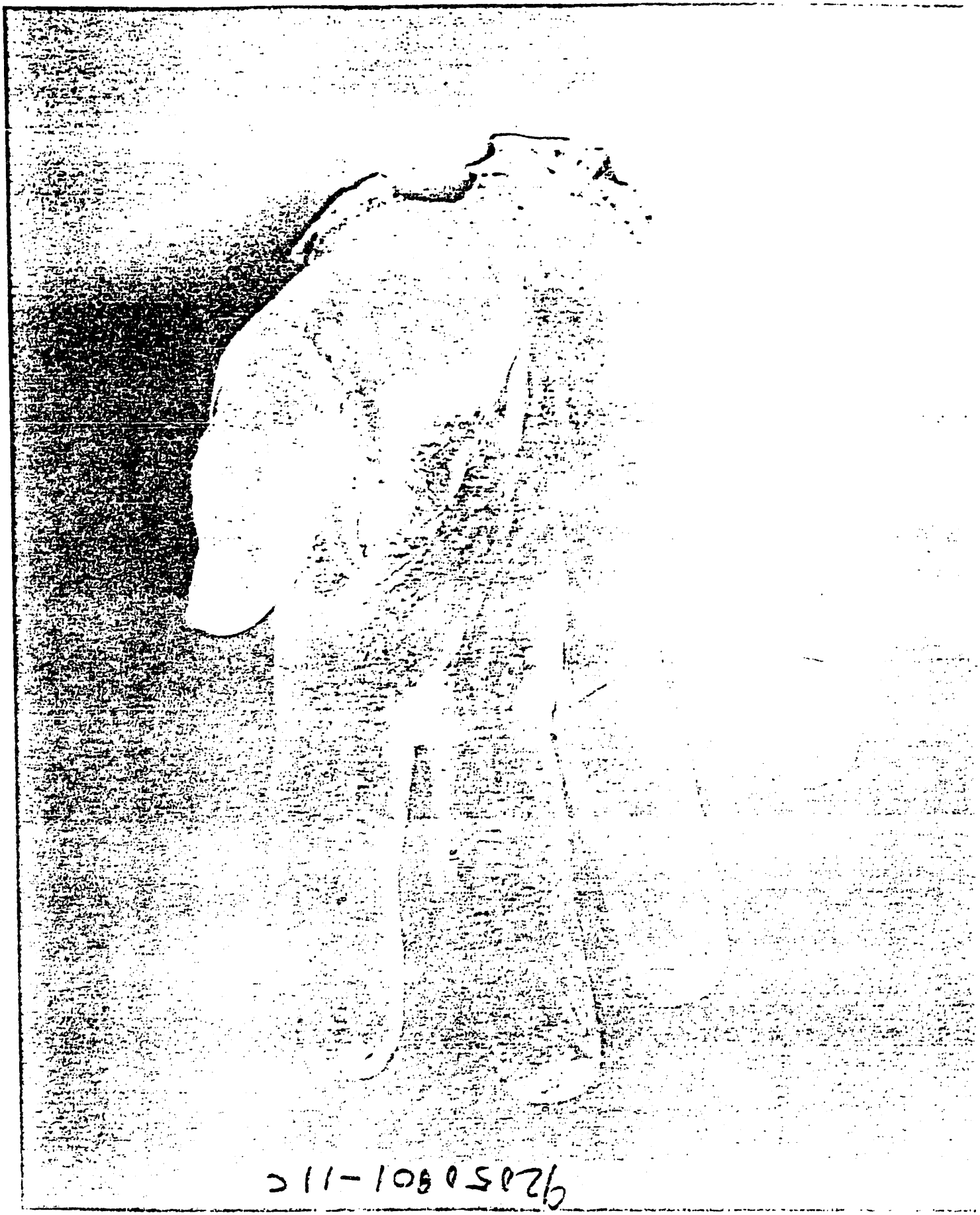
92050801-11c

PHANTOMS
MATERIALS

- requirements...
  - chemically inert to DALM
  - optically/RF transparent and non-scattering
- tested...
  - cyanoacrylate butyrate
  - polyethylene teraphthalate
  - cellulose acetate butyrate
  - epoxies
  - silicone
- using...
  - DOW 334 epoxy
  - Texaco Jeffamine 403 hardener

PHANTOMS
CURRENT/NEAR FUTURE

- thin (2-3 mm) shells in general
- human hand(s)
- human head
- human limbs
- rat (with and without imbedded skeleton)

UPGRADES

- camera sensitivity
- camera dynamic range (12-16 bit)
- RF/thermal/optical system integration
- laptop portability
- computing power/speed
- networking

SUMMARY...

- QLIS - delivered, upgraded, in use
- M-QLIS - delivered, improvement required
- L-QLIS - delivered
- Phantoms
  - thick hand delivered; thin hand delivered
  - mid-thickness hand imminent
  - head or rat next
- RF M-QLIS Radiator - delivered
- Upgrades - computers, peripherals, cameras
- Current Development - 3-D, portable, integration

END

DATE FILMED

8/11/93